

Document downloaded from:

<http://hdl.handle.net/10251/151275>

This paper must be cited as:

Aldas-Carrasco, MF.; Ferri, JM.; López-Martínez, J.; Samper, M.; Arrieta, MP. (2020). Effect of pine resin derivatives on the structural, thermal, and mechanical properties of Mater-Bi type bioplastic. *Journal of Applied Polymer Science*. 137(4):1-14.  
<https://doi.org/10.1002/app.48236>



The final publication is available at

<https://doi.org/10.1002/app.48236>

Copyright John Wiley & Sons

#### Additional Information

"This is the peer reviewed version of the following article: Aldas, M., J. M. Ferri, J. Lopez-Martinez, M. D. Samper, and M. P. Arrieta. 2019. Effect of Pine Resin Derivatives on the Structural, Thermal, and Mechanical Properties of Mater-Bi Type Bioplastic. *Journal of Applied Polymer Science* 137 (4). Wiley: 48236. doi:10.1002/app.48236, which has been published in final form at <https://doi.org/10.1002/app.48236>. This article may be used for non-commercial purposes in accordance with Wiley Terms and Conditions for Self-Archiving."

**The effect of pine resin derivatives on the structural, thermal and mechanical properties of Mater-Bi® type bioplastic**

M. Aldas<sup>a,b,\*</sup>, J. M. Ferri<sup>b</sup>, J. Lopez-Martinez<sup>b</sup>, M. D. Samper<sup>b</sup>, M. P. Arrieta<sup>c,\*</sup>

<sup>a</sup> Departamento de Ciencia de Alimentos y Biotecnología, Facultad de Ingeniería Química y Agroindustria, Escuela Politécnica Nacional, 170517 Quito, Ecuador

<sup>b</sup> Instituto de Tecnología de Materiales. Universitat Politècnica de València, 03801 Alcoy-Alicante, Spain

<sup>c</sup> Departamento de Química Orgánica, Facultad de Ciencias Químicas, Universidad Complutense de Madrid, Avenida Complutense s/n, Ciudad Universitaria, 28040 Madrid, Spain.

\* Corresponding author: Miguel Aldas, Marina P. Arrieta

E-mail: miguel.aldas@epn.edu.ec; marina.arrieta@gmail.com

Postal address:

Laboratorio C1L2

Instituto de Tecnología de Materiales. Universitat Politècnica de València.

Plaza Ferrandiz y Carbonell nº 1,

03801 Alcoy (Alicante), Spain

Tel.: (+34) 64 474 75 47

Fax: (+34) 96 652 84 78

## **Abstract**

The effect of three additives derived from pine resin: gum rosin (GR) and two pentaerythritol ester of gum rosin, Lurefor (LF) and Unik Tack (UT) in 5, 10 and 15 wt.%, on the properties of Mater-Bi®, based on plasticized starch, poly(butylene adipate-co-terephthalate) (PBAT) and poly( $\epsilon$ -caprolactone) (PCL) obtained by injection moulding processes was studied. The mechanical, microstructural and thermal properties were evaluated. LF had a cohesive behaviour with the components of Mater-Bi®, increasing the toughness of the material up to 250% accompanied by an increase of tensile modulus and tensile strength. UT had an intermediate behaviour, conferring cohesive and plasticizing effects, allowing an increase of 105% in impact resistance. GR had a more marked plasticizing effect. This allows processing temperatures of about 50 °C lower than those used for neat Mater-Bi®. Also, an increase of the elongation at break, toughness and impact resistance in 370%, 480% and 250%, respectively, was achieved.

**Keywords:** Biodegradable polymers; Thermoplastic starch; Gum rosin; Pine resin derivatives, Compatibilizer; Plasticizer.

## **1. Introduction**

The consumption of the “commodities” plastics has been growing during the last decades. In fact, the worldwide consumption in 2016 of only thermoplastics, polyurethanes and thermosets was 335 million tonnes and 60 million in Europe.<sup>1</sup> The worldwide concern for the generation of high amounts of plastic waste, added to the

environmental impact caused by traditional plastics after their useful life has motivated the research on more environmentally friendly materials.<sup>2</sup> Not only in those plastics that are biodegradables, but also in those that comes from renewable sources.<sup>3-5</sup> As a consequence, bio-polymers are gaining interest in several industrial applications. Thus, the research on polymeric materials that combine both properties, biobased sources and biodegradable character, such as polylactides (polylactic acid, PLA), the family of poly(hydroxyalkanoates) (PHAs), proteins (caseinates, soya) as well as polysaccharides (i.e.: chitosan, pectins, ligno-cellulosic products, gums, starch, etc.) among others, has been increasing in recent years.<sup>3,6-11</sup> Among the bio-based polymers currently commercialized, those derived from agro-resources, such as starch and in particular in its thermoplastic form, are the most widespread and economic bio-polymers.<sup>12-14</sup> In fact, the introduction of starch in the plastic sector has been motivated by its low cost due to the fact that it is available in large quantities. However, starch cannot be processed through conventional processing plastic techniques without further modification since its degradation begins at a temperature lower than its melting point.<sup>8</sup> Therefore, its thermoplastic form, thermoplastic starch (TPS), has gaining considerably interest in several industrial sectors in which biodegradability is a key factor, including the packaging industry, disposable products for hygienic and sanitary uses, etc.<sup>15</sup> However, the development of TPS-based materials is still limited due to its fragility, low water resistance and dependence on the mechanical properties on the environmental moisture.<sup>16,17</sup> In fact, it is widely known that, bioplastic materials may have lower performance than traditional synthetic plastics due to their inherent characteristics.<sup>6,18-20</sup> This is why TPS has also been blended with other polymers with a view to widening its range of applications<sup>13,21</sup>, as in the case of bags produced in association with PCL by extrusion displaying low-density polyethylene-like mechanical performance.<sup>14</sup>

Therefore, to obtain real alternatives to traditional synthetic polymers it is essential to improve their overall performance, so that novel formulations based on biopolymers will compete with traditional synthetic ones.<sup>20</sup> The plastic processing industry frequently modified the final properties of the polymers with additives, which are gradually replaced by natural ones, due to their advantages in terms of their lower environmental impact.<sup>22-24</sup> In this sense, Novamont commercializes blends based on TPS with biologically degradable polyesters under the trade name Mater-Bi®. Moreover, from both technical and environmental points of view, there is an increased interest on the use of agricultural biomass resources for the development of high-tech materials.<sup>2</sup>

On the other side, materials with natural origin such as resins derived from pine trees, that has been used since prehistory,<sup>25</sup> result interesting for the bioplastic industry.<sup>22,23</sup> In this sense, gum rosin and its derivatives has gained a renewed attention for the plastic field during the last years, as a source of monomer for polymer synthesis<sup>26</sup> and as additives (i.e.: stabilizers, plasticizers, viscosity increasing agents, nanoparticles modifiers, etc.).<sup>10,22,23,27</sup> Two products can be obtained after the resin, or gum, first distillation: “gum rosin” and “gum turpentine”. Resin production is a defensive response of the conifers to external factors such as bark boring insects and fungal pathogens, that can be induced by external factors (i.e.: mechanical wounding, abiotic stress, hormones and chemical stimulants or insect attack).<sup>25</sup> Most of gum rosins are composed mainly by abietic, levopimaric and pimaric acids,<sup>24,28,29</sup> which are monocarboxylic acids with the empirical formula  $C_{20}H_{30}O_2$  and have conjugated double bonds and carboxylic acids.<sup>29,30</sup> However, gum rosin shows relatively low thermal stability for the plastic processing industry. In this sense, some chemical modifications, such as hydrogenation and esterification confer to gum rosin higher thermal stability.

Most common alcohols used to stabilize the gum rosin are pentaerythritol, triethylene glycol and glycerol.<sup>24,28,31</sup> Resin and its derivatives have been proposed as low-cost, sustainable, and easily obtainable additives for plastic field.<sup>22,30,32,33</sup> In fact, the natural resins have the viability to be used in both, thermoplastic and thermoset polymers, due to their reactivity centres, the carboxyl group and its double bonds.<sup>22,34,35</sup> Particularly, the resins employed in this work, Lurefor (LF) and Unik Tack (UT) have different content of carboxylic groups, so that they possess different acid number which will provide better thermal stability as well as different ability to react with the polymeric matrix. The revalorization of gum rosin derivatives as plastic additives is interesting not only due to their natural origin and their similar structure in rigidity to rigid petroleum chemicals,<sup>34</sup> but also since cleaning activities are required for good forest management practices in terms of fire risk.<sup>22</sup> In this sense, in a previous work a triethylene glycol ester of gum rosin (TEGR) was used as the natural viscosity-increasing agent for polyvinyl chloride (PVC).<sup>22</sup> Several plastisols with tuneable mechanical and thermal performance were obtained depending on the TEGR proportion used, resulting interesting for several industrial applications.

In this work, three natural additives derived from pine resin: gum rosin, and two pentaerythritol ester of gum rosin were used as Mater-Bi® additives in three different compositions to improve the processability of the blends and to obtain materials with a broader spectrum of properties. The formulations were melt-extruded and further processed by injection moulding, to simulate the most typical processing approaches currently used at industrial level for traditional plastics. The effect of pine resin derivatives type and loading on the novel Mater-Bi® based formulations in terms of structural, thermal and mechanical properties was studied to get information regarding the possible applications of these novel formulations at the industrial level.

## 2. Experimental

### 2.1. Materials

Mater-Bi® NF 866 based on thermoplastic starch (TPS) and aliphatic aromatic polyesters (PBAT and PCL) was supplied by Novamont SPA (Novara, Italy). As additives, three pine resins derivatives were used: gum rosin (GR), supplied by Sigma-Aldrich (Mostoles, Spain); Lurefor 125 resin (LF, softening point of 125 °C and acid number 11.9), kindly supplied by LureSA (Segovia, Spain); Unik Tack P100 resin (UT, softening point of 90 °C and acid number 15), kindly supplied by United Resins (Figueira da Foz, Portugal).

### 2.2. Preparation of Mater-Bi®-resin formulations

The resin contents added to the Mater-Bi® matrix were 5, 10 and 15 wt.% and ten Mater-Bi®-resin based formulations were obtained, as shown **Table 1**. Initially, all materials were dried at 50 °C for 24 hours in an air circulation oven. Subsequently, the Mater-Bi®-resin formulations were premixed in plastic containers. Finally, to process the materials the following procedure was followed: (1) extrusion of the material formulations, (2) milling into pellets and (3) injection moulding to obtain test specimens. The materials were processed in a twin-screw extruder (Dupra S.L, Castalla, Spain), with a temperature profile of: 160 °C, 150 °C, 140 °C, 100 °C (from die to hopper) at 50 rpm. An injection moulding machine (Sprinter-11, Erinca S.L., Barcelona, Spain) was then used to obtain injection moulding test specimens. In this work, the

injection moulding process parameters were varied for each formulation by trial-and-error practice until good quality injected moulded test samples were obtained. Therefore, the injection moulding temperature profiles varied considerably in each group of formulations and are detailed in **Table 1**. The test specimens were standard rectangular specimens (80 x 10 x 4 mm) and standard tensile specimens “1BA” (length  $\geq 75$  mm, with 10 mm and thickness  $\geq 2$  mm) according to UNE-EN ISO 527.<sup>36</sup> Starchy materials are water sensitive and it has been observed that TPS based materials performance are influenced by the humidity (i.e.: mechanical<sup>37</sup> and thermal<sup>38</sup> properties). Therefore, all samples were conditioned 24 h at  $25\pm 1$  °C and  $50\pm 5\%$  HR previous to be characterized.

**Table 1.** Mater-Bi®-resin formulations and their injection moulding temperature profiles

Formulation labelling	Resin content in each formulation (wt.%)	Injection moulding temperature profiles (from die to hopper) (°C)
Mater-Bi®	0	165, 160, 160
MaterBi-5LF	5	165, 160, 160
MaterBi-10LF	10	150, 150, 145
MaterBi-15LF	15	145, 140, 135
MaterBi-5UT	5	150, 145, 140
MaterBi-10UT	10	150, 145, 140
MaterBi-15UT	15	120, 115, 105



MaterBi-5GR	5	130, 125, 115
MaterBi-10GR	10	117, 112, 100
MaterBi-15GR	15	117, 117, 105

---

### 2.3. ATR-FTIR characterization

All developed materials as well as the starting raw materials (pine resins and Mater-Bi®) were characterized by Attenuated total reflectance - Fourier Transform Infrared Spectroscopy (ATR-FTIR), using a Perkin Elmer – Spectrum BX (FT-IR system) within the range of 4000 to 650  $\text{cm}^{-1}$ , with a resolution of 4  $\text{cm}^{-1}$  and 32 scans. FTIR of resins were recorded using KBr discs made by blending the resins and KBr powder in transmission mode. FTIR of Mater-Bi® and Mater-Bi®-resin formulations were obtained from the injected samples.

### 2.4. Mechanical characterization

The tensile and flexural properties of the Mater-Bi®-resin based formulations were assessed in a universal test machine Ibertest Elib 30 of SAE Ibertest (Madrid, Spain) at room temperature, according to ISO 527<sup>36</sup> and ISO 178,<sup>39</sup> respectively. The tests were performed with a loading cell of 5 kN and a test speed of 10  $\text{mm min}^{-1}$ . At least five specimens from each formulation for both, tensile strength as well as for flexural measurements, were tested. In addition, to analyse the toughness of the materials, the area under the typical stress-strain curve and the increase of toughness with respect to the neat Mater-Bi® were calculated. For each sample, one curve was

chosen to be representative of the average behaviour of each formulation.<sup>20</sup> The area was calculated using the OriginPro2015 program.

The resistance to the Charpy Impact by drop of pendulum was measured in a Metrotec S.A. machine (San Sebastian, Spain), using a 1 J pendulum and notched specimens under the ISO 179<sup>40</sup>. The geometry of the notch was type A, with a background radius of  $0.25 \pm 0.05$  mm, the remaining width of  $8.0 \pm 0.2$  and the notch angle was  $45^\circ \pm 1^\circ$ . At least five specimens were tested, and the mean was reported.

Shore D hardness of samples with 4 mm thickness was measured on a durometer Model 673-D from Instrument J.Bot S.A. (Barcelona, Spain), under the ISO 868.<sup>41</sup> The mean of at least 20 measurements was reported as the hardness values.

Significance in the mechanical data differences were statistically analyzed with OriginPro 8 software. One-way analysis of variance (ANOVA) was carried out and significant differences among formulations were recorded at 95% confidence level according to Tukey's test.

## 2.5. Microstructural characterization

Scanning electron microscopy (SEM) micrographs from the fracture surface of the impact specimens were obtained using a Phenon SEM equipment of FEI (Eindhoven, The Netherlands) with a voltage of 5 kV and using a working distance for 1000 X and 5000 X of 241  $\mu\text{m}$  and 48  $\mu\text{m}$ , respectively. Previously, the samples were coated with a gold-palladium alloy to make their surface conductive, on a Sputter Mod Coater Emitech SC7620, Quorum Technologies (East Sussex, UK).

## 2.6. Thermal characterization

DSC experiments were conducted in a DSC 2000 calorimeter TA Instruments (New Castle, USA) under nitrogen atmosphere (50 mL min<sup>-1</sup>). Samples were subjected to a thermal cycle consisting in a first heating stage from -60 °C to 190 °C, to remove thermal history; followed by a cooling process down to -60 °C and subsequent heating up again to 190 °C, all scans at a heating rate of 10 °C min<sup>-1</sup>. The degree of crystallinity ( $X_c$ ) of the formulated materials was evaluated according to equation 1 and considering PBAT the most abundant polymeric fraction in Mater-Bi® of 70 wt.%.<sup>5</sup>

$$X_c(\%) = \frac{\Delta H_m - \Delta H_{CC}}{f \times \Delta H_m^c} \times 100 \quad (1)$$

Where  $\Delta H_m$  is the melting enthalpy and  $\Delta H_{CC}$  is the cold crystallization enthalpy of PBAT.  $\Delta H_m^c$  is the calculated melting enthalpy of purely crystalline PBAT, being 114 J/g.<sup>42</sup>

Thermogravimetric analysis (TGA) was conducted in TGA Q500 thermal analyser TA Instruments (New Castle, USA). Samples were heated under TGA dynamic mode from 55 °C to 700 °C at 10 °C min<sup>-1</sup> under nitrogen atmosphere (flow rate 50 mL min<sup>-1</sup>). The onset degradation temperatures ( $T_{5\%}$ ) were determined at 5% of mass loss, while temperatures of the maximum decomposition rate ( $T_{max}$ ) were calculated from the first derivative of the TGA curves (DTG).

The Heat Deflection Temperature (HDT) was determined using a VICAT/HDT station DEFLEX 687-A2, Metrotec SA (San Sebastián, Spain) according to ISO 75 (method A)<sup>43</sup> applying a force of 1.8 MPa with a heating rate of 120 °C h<sup>-1</sup>.

Dynamic mechanical thermal analysis (DMTA) in torsion mode was done on rectangular samples sizing  $40 \times 10 \times 4$  mm, in an oscillatory rheometer AR G2 from TA Instruments (New Castle, USA) equipped with a special clamp system for solid samples. The temperature of the test was from  $-50$  °C to  $110$  °C at a heating rate of  $2$  °C  $\text{min}^{-1}$  at a frequency of  $1$  Hz and  $0.1\%$  of maximum deformation.

### 3. Results

#### 3.1. Processing behaviour

The determination of the process parameters for injection moulding is highly skilled task and it is mainly based on a intuitive sense during the preparation of the formulations by the skilled operator's "know-how" acquired through long-term experience.<sup>44</sup> In this work, as reports **Table 1** during the samples preparation with each pine resin derivative, it was necessary to change the temperature profile to achieve optimal fill of the mould for the injection moulding process. Although to scale up the injected moulded materials developed here for their commercial production the process optimization is required, including a proper experimental design instead of trial-and-error practice, some interest aspects were observed during materials processing. For instance, the profile of temperature on the injection moulding process vary considerably, from  $165$  °C in die of the machine for neat Mater-Bi®, to  $145$  °C,  $120$  °C and  $117$  °C for MaterBi-15LF, MaterBi-15UT and MaterBi-15GR, respectively. Hence, it is possible to point out the effect of pine resin derivatives on the injection moulding processing properties of the Mater-Bi®. This drop of temperature is related to the reduction of softening point of resins and it could help to save energy when processing, very interesting for their processing at industrial level. Moreover, this effect could be

interesting in materials that have a narrow processing window or when high processing temperatures are not allowed, to prevent the materials thermal degradation.<sup>3,6,33</sup>

### 3.2. FTIR characterization

**Figure 1** shows the FTIR spectra of all developed materials as well as the starting raw materials (pine resins and Mater-Bi®). Mater-Bi® exhibits a peak at 2915  $\text{cm}^{-1}$  corresponding to C-H stretching in aliphatic and aromatic groups; others at 1724  $\text{cm}^{-1}$  and 1250  $\text{cm}^{-1}$  due to the carbonyl groups (C=O) and the C-O link respectively, found in the ester linkage.<sup>14</sup> A group of peaks reported at 1578, 1504, 1458 and 1022  $\text{cm}^{-1}$  attributed to stretching of phenylene groups and at 728  $\text{cm}^{-1}$  a peak attributed to four or more adjacent methylene (-CH<sub>2</sub>-) groups. Finally, bending peaks of the benzene substitutes are located between 900 and 700  $\text{cm}^{-1}$ . All these groups are attributed to PBAT portion.<sup>5,45,46</sup> The plasticized starch portion of the Mater-Bi® results in peaks between 3900 - 3300  $\text{cm}^{-1}$ , attributed to O-H stretching; 1445 - 1325  $\text{cm}^{-1}$ , due to C-H bending and wagging and peaks between 1250-900  $\text{cm}^{-1}$  attributed to C-O stretching and hydrogen bonding peaks. The peaks at 1180 and 1104  $\text{cm}^{-1}$  correspond to C-O stretching of the C-O-H group (the starch group which mainly participates in hydrogen bonding). The peak at 1022  $\text{cm}^{-1}$  corresponds to C-O stretching of the C-O-C group of the starch anhydroglucose ring which also can participate in hydrogen bonding.<sup>47,48</sup> There are also PCL characteristic peaks which are due to C=O stretching (1724  $\text{cm}^{-1}$ ), symmetric CH<sub>2</sub> stretching (2853  $\text{cm}^{-1}$ ) and asymmetric CH<sub>2</sub> stretching (2952  $\text{cm}^{-1}$ ).<sup>49,50</sup> Thus, the commercial Mater-Bi® used in this study is based on PBAT, plasticized starch and PCL as well as other additives in less proportion, in well accordance with the

literature.<sup>5,45,46,48,49</sup> According to Borchani et al., the content of each polymer is about 70, 20 and 10 wt.%, respectively.<sup>5</sup>

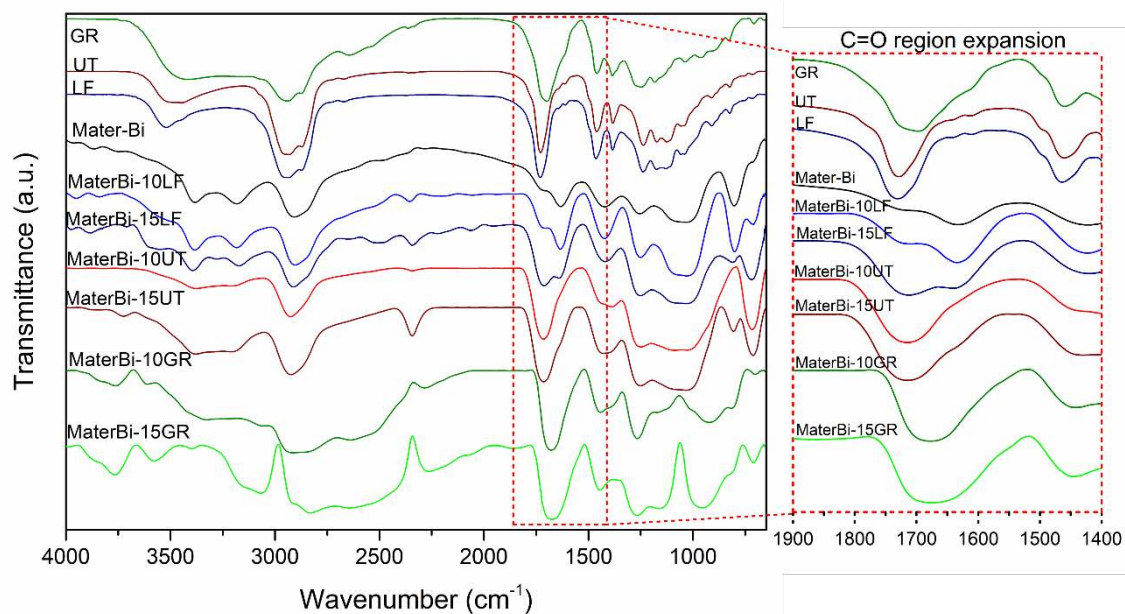


**Figure 1.** FTIR spectra of gum rosin (GR), pine resin derivatives (UT, LF), Mater-Bi®, and studied materials

FTIR spectra of gum rosin (GR) and its derivatives (LF and UT) shows common peaks around  $3500\text{ cm}^{-1}$  attributed to rosin, which after esterification in LF and UT showed two shoulders attributed to the appearance of O-H stretching of COOH in the resins, suggesting the presence of acids stabilizers in pentaerythritol ester resins and/or somewhat amount of resin in the form of gum rosin due to the incomplete reaction of pentaerythritol esters.<sup>29</sup> There are two peaks at  $2944\text{ cm}^{-1}$  and  $2872\text{ cm}^{-1}$  because of the C-H stretching. Also one peak at  $1698\text{ cm}^{-1}$ , attributed to hydrogen bonded acid dimers of gum rosin and to the C=O stretching of the gum rosin. This peak corresponding to the carboxylic acids groups has been slightly shifted to  $1730\text{ cm}^{-1}$  in LF and UT. Peaks at

1450  $\text{cm}^{-1}$  are due to  $\text{CH}_2$  bending mode, 1362  $\text{cm}^{-1}$  are due to  $\text{CH}_3$  bending, while those at 1225  $\text{cm}^{-1}$  and 1215  $\text{cm}^{-1}$  are due to the C-O stretching of acid groups. Finally, some peaks from 1000 to 650  $\text{cm}^{-1}$  correspond to C-H out of plane bending.<sup>30,51,52</sup>

Regarding formulated materials, the peaks observed for the raw starting materials are also observed in the formulations. In LF based formulations, the peak at 3390  $\text{cm}^{-1}$ , attributed to O-H stretching of TPS,<sup>12</sup> increase its intensity. Meanwhile the peaks at 2915  $\text{cm}^{-1}$  and 1724  $\text{cm}^{-1}$  of TPS were shifted to 2890  $\text{cm}^{-1}$  and 1710  $\text{cm}^{-1}$ , respectively suggesting somewhat positive interaction between the polymeric matrix and the resin. The intensity of the peak corresponding to C-H stretching in aliphatic and aromatic groups (2915  $\text{cm}^{-1}$ ) decrease when the content of resin increase. As expected, the intensity of the carbonyl groups (C=O) and the C-O link increase with the resin content, due to the increment of the esters linkage coming from the resin, while the shift to lower wavelengths suggest hydrogen bonding interactions (see the expansion of the spectra in the C = O stretching region in Figure 1). Moreover, the intensity of peaks between 1250 and 800  $\text{cm}^{-1}$  increase their value when the resin content increase, due to the increment of C-O stretching and also probably due to the formation of hydrogen bonding interaction between Mater-Bi® hydroxyl groups and the resin carbonyl groups. Finally, the peak corresponding to benzene substitutes (718  $\text{cm}^{-1}$ ) also increase with the resin content due to the chemical structure of the resin, then again confirming the correct incorporation of the LF resin into the polymeric matrix. Similar findings have been found for UT based formulations, because both resins are gum rosin esters. For instance, the peak corresponding to the carbonyl group (C=O) was shifted from 1724  $\text{cm}^{-1}$  to 1716  $\text{cm}^{-1}$  suggesting hydrogen bonding interactions (see the expansion of the spectra in the C = O stretching region in Figure 1). On the other hand, the main difference with GR based formulations is that the peaks at 1710 and 1638  $\text{cm}^{-1}$  are

merged in a bigger one centered at  $1680\text{ cm}^{-1}$ , probably due to the less hydrogen bonding interactions previously commented for other additives (see the expansion of the spectra in the C = O stretching region in Figure 1).

These FTIR spectra revealed that the molecular structure of the additives (gum rosin and its derivatives) interacts with that of the Mater-Bi® during the formulation of materials. The spectra of both materials, that is the polymeric matrix and the resin, are well merged in the studied formulations. This phenomenon suggests a good chemical interaction such as the formation of hydrogen bonds between each resin and the components of the polymeric matrix, particularly in the case of pentaerythritol esters of gum rosin, as it has been previously observed when using gum rosin derivatives as polymer additives.<sup>22,23,30,52</sup>

### 3.3. Mechanical properties

The tensile properties of materials were evaluated, and it was observed that neat Mater-Bi® has a tensile strength of 8.2 MPa, tensile modulus of 239 MPa and an elongation at break of 18.4%. **Figure 2-a** and **2-b** represents the variation of Young's modulus and tensile strength in terms of percentage and type of resin. The incorporation of LF and UT resins up to 10 wt.% in the blend, did not significantly ( $p < 0.05$ ) modify the Young's modulus while the tensile strength slightly increased ( $p > 0.05$ ), around 13% in MaterBi-10LF, compared to neat Mater-Bi®. This behaviour could be explained because of the modified resins make easier the compatibilization between the resin and the polymeric matrix,<sup>5</sup> in good accordance with the already commented hydrogen bonding interactions. For larger contents, that is 15 wt.% of LF, a significant increment of 14% of the modulus was reached ( $p > 0.05$ ). However, the maximum strength,



although higher than neat Mater-Bi®, did not show significant changes when LF resin content increases.

With UT resin, an intermediate effect between plasticizing and compatibilization was observed. As the resin content increases, the Young's modulus of the material tends to decrease, up to 20% lower in MaterBi-15UT ( $p > 0.05$ ) compared to the neat Mater-Bi®. The tensile strength for the MaterBi-5UT and MaterBi-10UT presented a slight significant ( $p > 0.05$ ) increment respect to neat matrix, showing the positive interaction between Mater-Bi® and UT resin probably due to the already commented hydrogen bonding interactions. However, a saturation effect is observed from contents of 5 wt.% of UT, where the higher value of tensile strength was achieved. The same effect was observed by Ferri et al. when using maleinized linseed oil as Mater-Bi® and PLA compatibilizer in ternary blends.<sup>6</sup> This effect makes that the maximum resistance significantly ( $p > 0.05$ ) drops from 9.3 MPa in the MaterBi-5UT to 7.6 MPa in MaterBi-15UT, which represents the maximum decrease (7.3%) of Mater-Bi® tensile strength. Borchani et al. also reported an increment in Young's modulus and tensile strength in Mater-Bi® by using Alfa fibers for the development of biocomposites, and they attributed this result to the good interfacial adhesion between Mater-Bi® and the fibers<sup>5</sup>. Therefore, it is possible to establish that the modified pine resins used in this work have a good compatibilization effect among the Mater-Bi® components, in good agreement with FTIR results.

A very different behaviour was observed in unmodified resin (GR) based formulations. The Young's modulus and maximum strength had a significant loss ( $p > 0.05$ ). Even though, the loss of tensile strength was not proportional to the resin content, since all three formulations experienced a loss of 28% with respect to the strength of the neat Mater-Bi®. In contrast, the Young's modulus showed a linear decrement

behaviour, reporting a loss of Mater-Bi® Young's modulus from a 40% up to 70% in the MaterBi-5GR and MaterBi-15GR, respectively. This effect caused by GR in tensile properties was also observed by Narayanan et al., in PLA/rosin materials.<sup>23</sup>

The elongation at break (**Figure 2-c**) increased regardless the type or content of pine resin suggesting a plasticizing effect, particularly in the case of the gum rosin. It is important to observe that with a content of 10 wt.% of any type of resin, the elongation at break was similar in all formulations, with a value of about 30%. This property remains constant with 15 wt% in the blends with LF and UT ( $p < 0.05$ ), while it increased in GR based formulations ( $p > 0.05$ ). In fact, MaterBi-15GR showed a significant increase of the elongation at break, from 18.4% in neat Mater-Bi® to 85.7% in MaterBi-15GR. This is an indicative of a plasticization effect, which let the reduction of processing temperature, as it was already discussed in the processing behaviour of Mater-Bi® and its blends. In all formulations, an increase in the cohesion of the material was observed, although this behaviour is different depending on the pine resin derivative. The LF and UT resins contribute to cohesion and higher resistance values. This is due to the compatibilizing effect they produce on the Mater-Bi® components.<sup>5,20</sup> In contrast, GR confers lower strength and Young's modulus and a longer elongation at break, an indicative of a marked solubilizing, compatibilizing and plasticizing effect, thus providing a greater ductility to the Mater-Bi®. Moreover, the solubility of GR with the polymeric matrix is considerably higher than the one for modified rosins, which allows a greater movement of the polymer chains and, consequently, a greater deformation and easier processability. In fact, in GR based formulations saturation is not reached as shown in **Figure 2-c**.

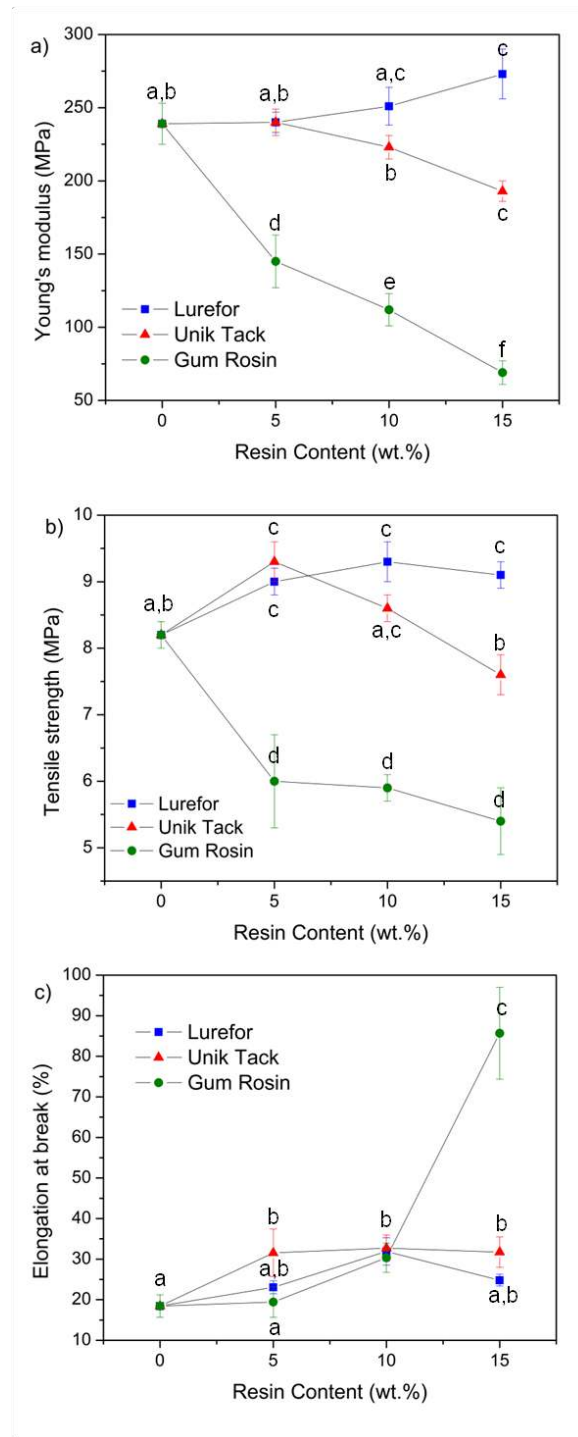


**Figure 2.** Effect of increasing amount of pine resin derivatives on the tensile properties of Mater-Bi®-based formulations a) Young's modulus, b) tensile strength and c) elongation at break.

<sup>a-f</sup> Different letters within the same graph indicate statistically significant differences between formulations ( $p < 0.05$ ).

Analysing the flexural properties, charted in **Figure 3**, materials formulated with LF did not showed significant ( $p < 0.05$ ) changes either in flexural modulus (**Figure 3-a**) or in maximum flexural strength (**Figure 3-b**). In contrast, the formulations with UT and GR experienced a significant ( $p > 0.05$ ) loss of both properties as their content increases. Specifically, flexural modulus and maximum flexural strength decreased by 38% and 72% respectively, compared to neat Mater-Bi® for materials containing 15 wt.% of UT ( $p > 0.05$ ); while decreased 27% and 54% respectively, for materials containing 15 wt.% of GR. This behaviour is due to the increase of the ductility, more marked in GR based formulations, produced thanks to the good solubility of this resin in the Mater-Bi® polymeric matrix. Such solubility promotes the lubricity of the polymer chains and therefore, an improved ductility. This phenomenon, also reported by Narayanan et al. in materials containing GR, plays an effective role in enhancing the elongation at break, providing suitable materials for industrial applications such as biodegradable films.<sup>23</sup>

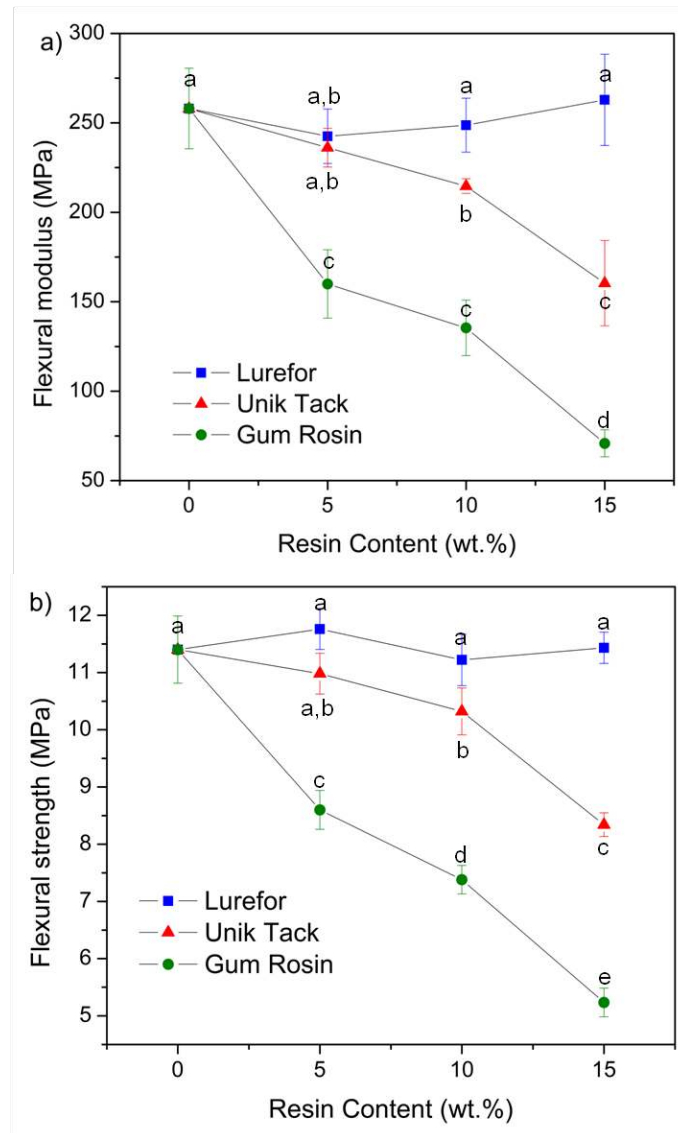


**Figure 3.** Effect of increasing amount of pine resin derivatives on the flexural properties of Mater-Bi®-based formulations a) flexural strength and b) flexural modulus.

<sup>a-e</sup> Different letters within the same graph indicate statistically significant differences between formulations ( $p < 0.05$ ).

Regarding the toughness of materials ( $T$ ), which is shown in **Table 2**, the toughness of all formulations increased considerably compared to neat Mater-Bi®, except for the MaterBi-5GR formulation, which remains similar to Mater-Bi®. However, results for MaterBi -15GR stands out because it showed an increase of toughness more than 450%

higher than the neat matrix. Regarding UT and LF, these resin derivatives provided greater cohesion to the Mater-Bi®, thus increasing their mechanical performance due to the interaction of the polar groups of the resins with the aliphatic and aromatic groups presents in the Mater-Bi®<sup>24</sup> as it was previously observed by Arrieta et al. in PVC-resin based materials.<sup>22</sup> UT resin seems to have a significant higher cohesive effect at lower contents (5 wt.%) than the LF resin, although with 10 wt.% of LF, MaterBi-10LF achieved greater toughness and ductility than MaterBi-10UT. Moreover, with GR addition, an increase of the ductility was also obtained, as a consequence of its greater plasticization effect.<sup>17</sup>

**Table 2.** Area of stress-strain curve (toughness) and its comparison with neat Mater-Bi® toughness.

Formulation	Toughness $T$ (kJ.m <sup>-3</sup> )	Increase of toughness (%)
Mater-Bi®	745	-
MaterBi-5LF	1388	86
MaterBi-10LF	2657	257
MaterBi-15LF	1514	103
MaterBi-5UT	2287	207
MaterBi-10UT	2141	187
MaterBi-15UT	1950	162
MaterBi-5GR	741	0
MaterBi-10GR	1227	65
MaterBi-15GR	4304	478

A deeper analysis of the stress-strain curve (**Figure 4**) shows that with a 10 wt.% of resin, the gain of Mater-Bi®-resin properties is much greater than that of the neat Mater-Bi®, since its earning rate of elongation, without losing Young's modulus. This behaviour is very outstanding for LF which showed the higher softening point, while it decreased for UT and GR based formulations in that order.

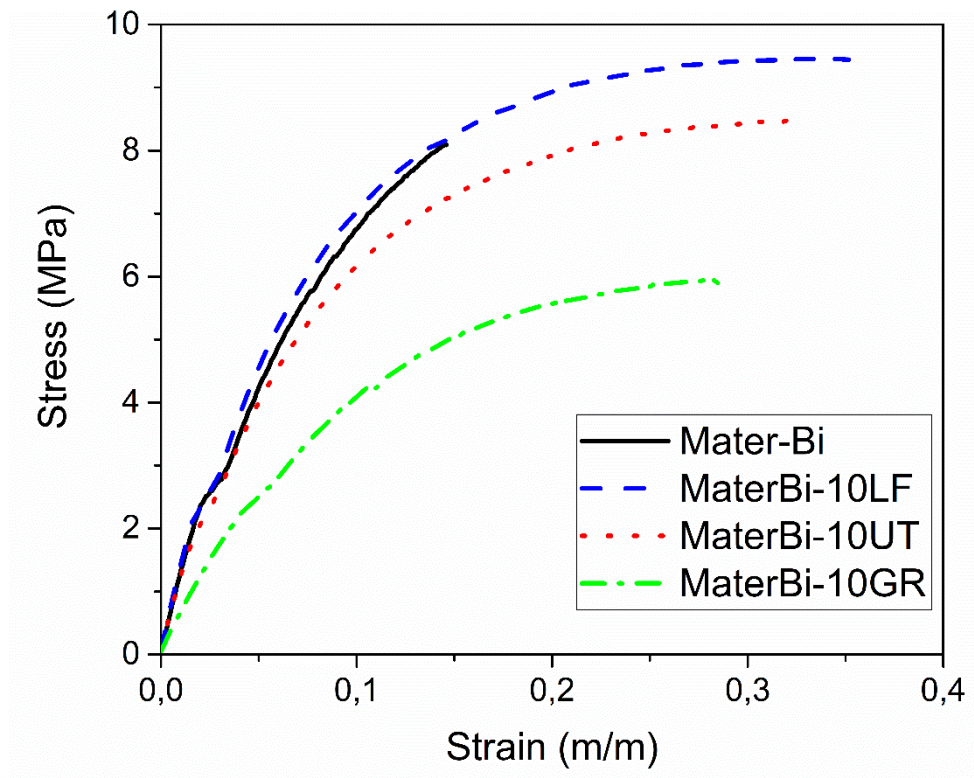


**Figure 4.** Stress-strain curve of neat Mater-Bi® and formulations with 10 wt.% of resin

Another property of the materials that gives an idea of the variation of the ductile properties is the impact absorption per unit area. As shown in **Table 3**, there are two clear trends: formulations added with UT and LF experienced a considerable significant ( $p > 0.05$ ) gain of energy absorbed at impact, although its saturation point is at low contents (5 wt.%). Whereas, formulations added with GR underwent a larger

increase than those provided by pentaerythritol esters of gum rosin (LF and UT). The increment is linear as the GR content increases, up to 250 % for MaterBi-15GR ( $p > 0.05$ ) respect to neat Mater-Bi®. This behaviour is related with the higher solubility of GR with Mater-Bi® resulting in a high increase of the ductility. This interaction confers high cohesion to the formulated material but low solubility of the resin in the Mater-Bi® matrix. The solubility behaviour between pine resin derivatives with the Mater-Bi® will be also confirmed by SEM observations, where it is possible to advise the reduction of the materials porosity (see section 3.4).

Regarding the hardness properties (**Table 3**), LF did not significant modify ( $p < 0.05$ ) Shore D hardness of the neat Mater-Bi®, regardless the content of resin. On the other hand, when using UT and GR, the hardness significant decreased ( $p > 0.05$ ), being very low in MaterBi-15GR in about 17% (lower compared to neat matrix).



1 **Table 3.** Variation of Charpy's impact energy, Shore D hardness and HDT of neat Mater-Bi® and Mater-Bi-resin formulations

	Charpy's impact energy			Shore D hardness			Heat deflection temperature HDT (°C)		
	(kJ/m <sup>2</sup> )								
Mater-Bi®	3,9±0.4 <sup>a</sup>			50.3 ± 0.6 <sup>a</sup>			35.6		
Rosin content	LF	UT	GR	LF	UT	GR	LF	UT	GR
(wt.%)									
5	7,8 ± 0.4 <sup>b</sup>	8.0 ± 0.8 <sup>b</sup>	3.8 ± 0.2 <sup>a</sup>	50.3 ± 1.0 <sup>a,b</sup>	50.0 ± 0.5 <sup>a,c</sup>	46.4 ± 0.6 <sup>e</sup>	33.8	34.5	32.8
10	6,9 ± 0.4 <sup>b,c</sup>	6.8 ± 0.3 <sup>c,d</sup>	8.0 ± 0.8 <sup>b,c</sup>	50.4 ± 1.0 <sup>a,b</sup>	49.6 ± 0.8 <sup>b,c</sup>	46.1 ± 0.6 <sup>e</sup>	31.3	25.6	*
15	5,2 ± 0.4 <sup>d,e</sup>	5.1 ± 0.3 <sup>a,e</sup>	13.8 ± 1.1 <sup>f</sup>	50.7 ± 0.7 <sup>a</sup>	48.7 ± 0.9 <sup>d</sup>	42.0 ± 0.8 <sup>f</sup>	34	*	*

\* HDT lower than room temperature (25 °C)

2 <sup>a-f</sup> Different letters within the same property indicate statistically significant differences between formulations (p < 0.05).

### 3 3.4. Scanning electron microscopy

4

5 The effect of pine resin derivatives on the microstructure of Mater-Bi® was  
6 studied by SEM. **Figure 5** and **Figure 6** show the SEM images of the fractured surface  
7 of neat Mater-Bi® and formulations blended with pine resin derivatives at low and high  
8 concentrations (5 wt.% and 15 wt.%), respectively.

9 A characteristic material with a lack of phase's cohesion is observed for neat  
10 Mater-Bi® (**Figure 5-a** and **Figure 6-a**). In addition, large discontinuities with flakes  
11 shape are observed, confirming this lack of cohesion due to a low miscibility between  
12 the components of the Mater-Bi® polymeric matrix (PBAT, plasticized starch and  
13 PCL). This morphology is also characteristic of ductile fractures in poor cohesion  
14 materials, mainly observed in binary or ternary blends with low miscibility (**Figure 5-**  
15 **a**).<sup>6,19</sup> Specifically, small spheres attributed to the minor portion of PCL are  
16 observed.<sup>53,54</sup> As well, plasticized starch domains are also observed and as a major  
17 component the PBAT portion.

18 In **Figure 5-b** and **c**, corresponding to the SEM micrographs of MaterBi-LF  
19 formulations, small domains of homogeneously distributed LF are observed. This  
20 morphology is due to the low solubility of this resin within Mater-Bi® matrix (**Figure**  
21 **5-b** and **Figure 6-b**), showing some “empty” interface between the two polymeric  
22 phases, suggesting a poor interfacial adhesion.<sup>54</sup> These domains increased with the  
23 increment of LF content (15 wt.% of resin, **Figure 5-c** and **Figure 6-c**). However, it is  
24 observed that the porosity of the material decreased considerably (**Figure 6-b**) with  
25 respect to neat Mater-Bi® (**Figure 6-a**). In addition, flakes due to lack of cohesion  
26 fracture were still observed, but these were smaller than those observed in the SEM  
27 images of Mater-Bi® matrix (**Figure 5-a** and **Figure 6-a**). Although the modified pine

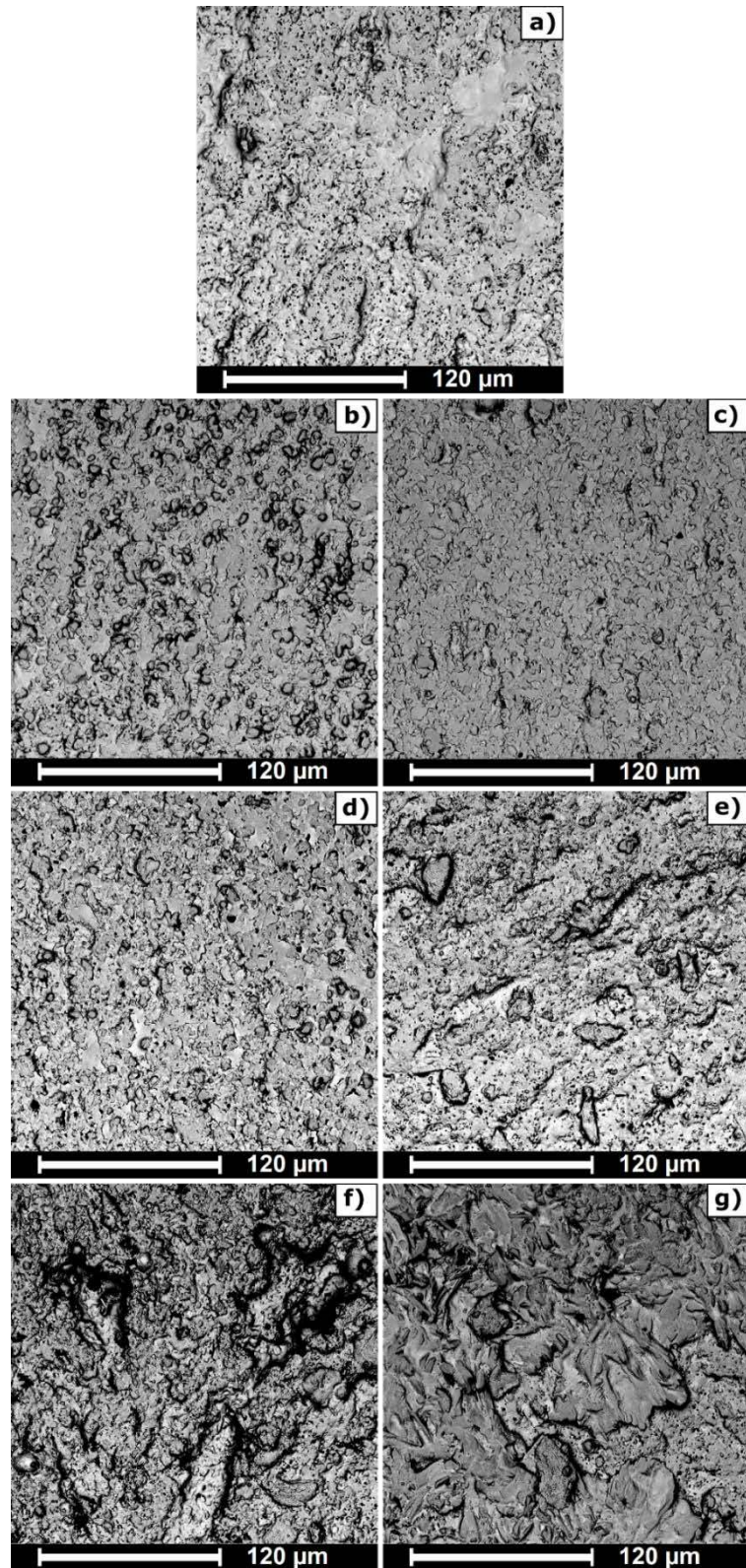
28 resins were not completely miscible with the components of Mater-Bi® (PBAT,  
29 plasticized starch and PCL), they may have a good interaction with some of those  
30 components and, consequently, they increase the cohesion of these components.<sup>3</sup>  
31 Therefore, it seems that LF confers a compatibilizing (cohesive) effect on the Mater-  
32 Bi®-based material, which was previously corroborated by the increase in tensile  
33 modulus and tensile strength, being higher for higher LF contents.

34 In **Figure 5-d** and **Figure 5-e** as well as **Figure 6-d** and **Figure 6-e**, the effect of  
35 the UT resin on the Mater-Bi® matrix is observed. As with LF, less porosity and  
36 smaller flakes were detected. In general, UT formulations show fewer discontinuities  
37 than the Mater-Bi® matrix (**Figure 5-a** and **Figure 6-a**). The morphology showed  
38 greater cohesion, which may be due to chemical interactions between UT resin and the  
39 components of the Mater-Bi® matrix.<sup>3,6,22</sup> This double effect, cohesive and plasticizing,  
40 can be corroborated with the evolution of the mechanical properties previously  
41 discussed; which, at low UT contents higher values in modulus and resistance were  
42 found, with respect to Mater-Bi®. However, for high UT contents (**Figure 5-e** and  
43 **Figure 6-e**), signs of a plasticizing effect were observed, in accordance with the  
44 increased elongation at break and reduced strength, Young's modulus and hardness, as  
45 reported in mechanical properties results.

46 Finally, in **Figure 5-f** and **Figure 5-g** as well as **Figure 6-f** and **Figure 6-g**,  
47 corresponding to the MaterBi-GR formulations, a very marked plasticizing effect confer  
48 by GR was observed. In these images, it is impossible to identify the different domains  
49 previously observed in neat Mater-Bi® (**Figure 5-a** and **Figure 6-a**), even more  
50 difficult for higher resin content (**Figure 5-g** and **Figure 6-g**). Thus, from the  
51 microstructure analysis it is possible to state that MaterBi-GR based formulations  
52 resulted in the most compatibilized samples. The discontinuities of the material are

53 considerably reduced. This behaviour results from the high affinity of the GR with the  
54 Mater-Bi® components. The small size of the GR molecules together with its reactivity  
55 centres, the carboxyl group and its double bonds<sup>22,35</sup> allowed GR to be solubilized in the  
56 intramolecular free volume of the Mater-Bi® polymeric matrices. In addition, the free  
57 volume increases and this behaviour contributes to an important increase in the  
58 miscibility between the components of the Mater-Bi® (PBAT, plasticized starch and  
59 PCL) and GR.<sup>6</sup> Thus, GR shows a plasticizer-compatibilizing effect, as it was also  
60 reflected in the reduction of the processing temperature as well as the mechanical  
61 performance, characterized by an increase in elongation at break, a significant decrease  
62 in strength and hardness, as well as an important increment in the impact energy.

63

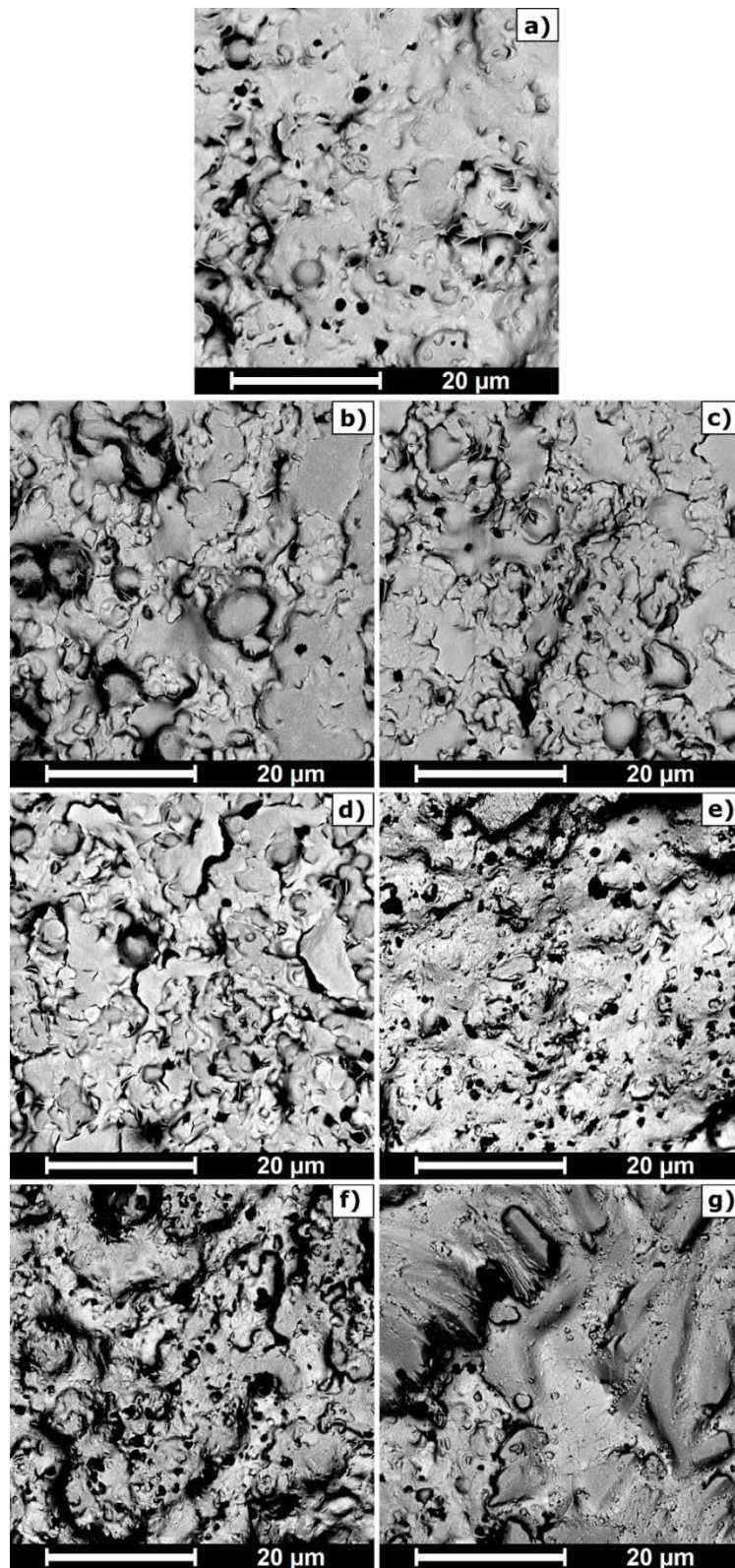


64

65 **Figure 5.** SEM images from impact fracture surface at 1000 X of: **a)** neat Mater-Bi®,

66 **b)** MaterBi-5LF, **c)** MaterBi-15LF, **d)** MaterBi-5UT, **e)** MaterBi-15UT, **f)** MaterBi-

67 **5GR** and **g)** MaterBi-15GR



68

69 **Figure 6.** SEM images from impact fracture surface at 5000 X of: **a)** neat Mater-Bi®, **b)**

70 MaterBi-5LF, **c)** MaterBi-15LF, **d)** MaterBi-5UT, **e)** MaterBi-15UT, **f)** MaterBi-5GR and

71

**g)** MaterBi-15GR.

### 72 3.5. Thermal properties

73

74 **Figure 7** shows the DSC second heating curves as well as the DSC cooling  
75 curves of samples added with 15 wt.% of pine resin as example to show the DSC  
76 changes more clearly. In addition, the thermal data of all formulations are summarized  
77 in **Table 4**. Mater-Bi® exhibited a thermal transition at -32 °C, corresponding mainly to  
78 the glass transition of the PBAT fraction ( $T_{gPBAT}$ ) with a combination of the  $T_g$  of the  
79 plasticized starch fraction ( $T_{gplasticized\ starch}$ ) of the Mater-Bi®.<sup>5,55,56</sup> In addition, Mater-  
80 Bi® presents a thermal transition at 56.3 °C, attributed to the PCL melting.<sup>50,53,57</sup> Due to  
81 the PCL content in Mater-Bi® is estimated to be less than 10 wt.%,<sup>5</sup> this thermal  
82 transition is very trivial, and no melting peak is observed. Moreover, the calorimetric  
83 curve of Mater-Bi® presents a cold crystallization peak at 107.3 °C, attributed to the  
84 cold crystallization of the PBAT portion. Finally, it is possible to determine two groups  
85 of melting peaks: one at 124.7 °C, corresponding to the melting of PBAT fraction,<sup>55</sup> and  
86 other two peaks centred at 150.3 °C attributed to the melting of the plasticized starch  
87 fraction.<sup>18</sup> The DSC cooling assessment in Mater-Bi®, shown in **Figure7-b**, exhibits a  
88 peak at 92.5 °C attributed to the crystallization of the PBAT fraction. This peak was also  
89 observed by Borchani et al., who used a similar Mater-Bi® in their study,<sup>5</sup> and by  
90 Lendvai et al.<sup>19</sup> and Muthuraj et al.<sup>55</sup>, who worked with TPS-PBAT blends and with an  
91 hydrolytically degraded PBAT, respectively. The  $T_{gPCL}$ , established between -40 and -  
92 60 °C,<sup>50,53,58</sup> could not be observed, possibly due to the low content of PCL in the  
93 Mater-Bi® (estimated to be less than 10 wt.%).<sup>5</sup>

94 Regarding the changes in the glass transition temperature, results showed that the  
95 effect of resins in Mater-Bi® is to slightly increase it. LF and UT resins increased the  $T_g$   
96 in about 5 °C when using 15 wt.% content of resin. Meanwhile, GR increased the  $T_g$  in

97 about 10 °C at the same percentage. Due to this  $T_g$  is attributed to the PBAT portion of  
98 Mater-Bi® the trend suggests that all additives used in this work are thermodynamic  
99 compatible with this component of the Mater-Bi®.<sup>59</sup> Moreover, the shift of  $T_g$  to high  
100 temperatures could show that PBAT interacts with the plasticized starch portion of the  
101 material with the aid of pine resins; thus, it increases the miscibility of these two  
102 portions confirming the compatibilizing and plasticizing effect of resins.

103       Regarding the melting temperature corresponding to PCL portion ( $T_{mPCL}$ ),  
104 typically in the range of 40 and 60 °C,<sup>50,53,60</sup> the pine resin derivatives slightly modify it.  
105 A shift to low temperatures was detected, due to the interaction of the resins with the  
106 PCL portion of Mater-Bi®. The PCL is also plasticized with the pine resin derivatives;  
107 even if this effect is light detectable in DSC, because the content of this portion is lower  
108 than 10 wt.%.<sup>5</sup> In addition, it is possible to notice that GR has an important effect on the  
109 PCL portion as showed the decreasing trend of the  $T_{mPCL}$ .

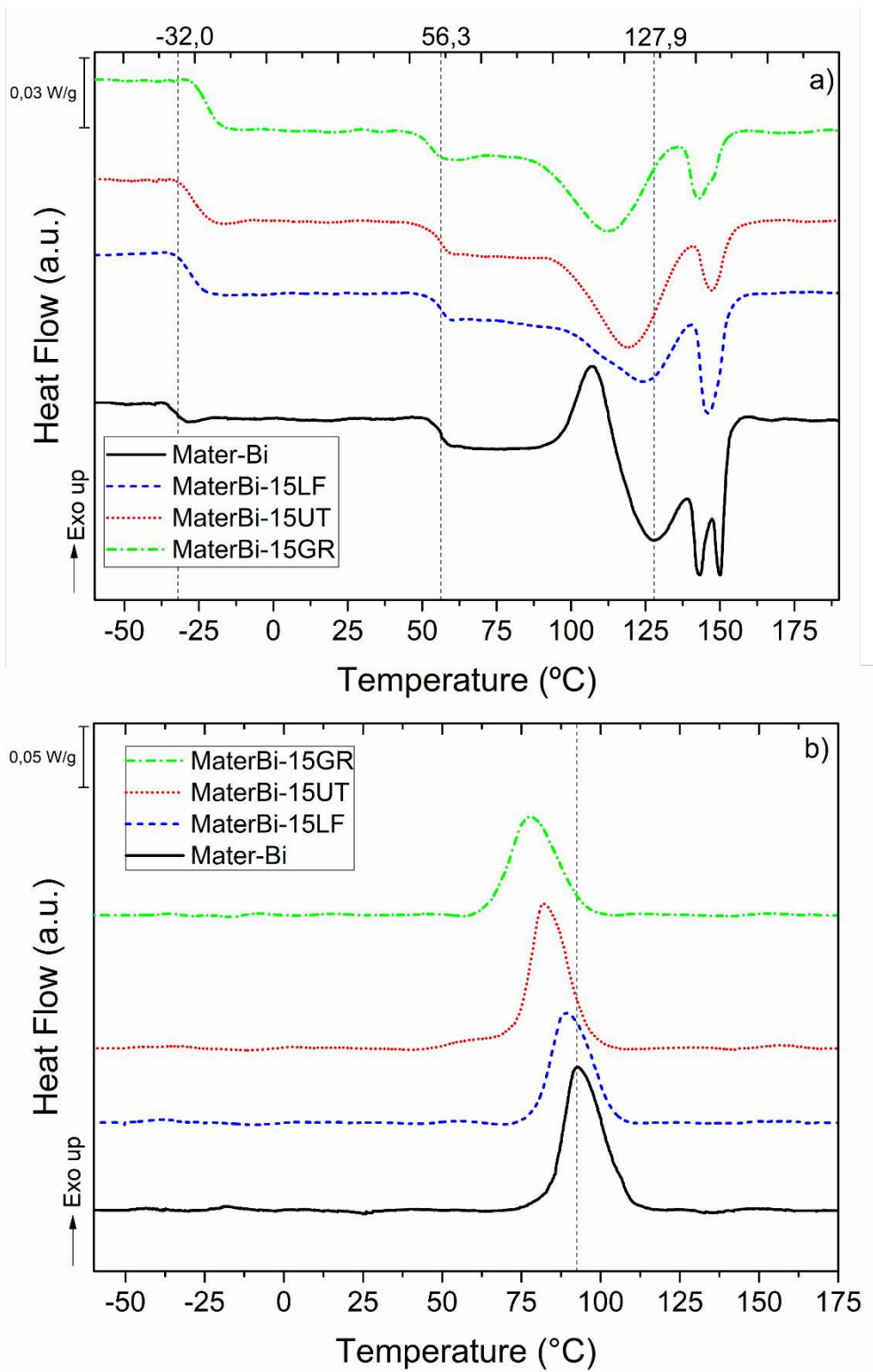
110       The cold crystallization peak present in neat Mater-Bi® ( $T_{cc}$ ) disappeared in all the  
111 formulations studied, suggesting that all the resin based formulations were able to  
112 promote the complete crystallization of the PBAT fraction at the low cooling rate  
113 applied. In fact, while the  $\Delta H_c$  and the  $\Delta H_m$  of PBAT was mainly maintained in neat  
114 MaterBi®, the degree of PBAT crystallinity increased for all resin based formulations.  
115 Concerning the melting temperature of PBAT portion ( $T_{mPBAT}$ ) there was a noticeable  
116 decrement of this temperature with all resin derivatives, mainly when using UT and GR.  
117 The variation on this temperature reaches 16 °C in MaterBi-15GR formulation.  
118 Moreover, analysing the tendency of the melting enthalpy of the PBAT portion  
119 ( $\Delta H_{mPBAT}$ ), it increased as the pine resin content increased in the formulation, regardless  
120 of the type of additive used. All these behaviours show that pine resin derivatives cause  
121 an important plasticizing effect on the base polymeric matrix, more specifically with the



122 PBAT portion of the Mater-Bi®. Furthermore, this behaviour suggests that all the pine  
123 resin derivatives studied are compatible with PBAT fraction of the Mater-Bi®.<sup>5,18,19,59</sup>  
124 Analysing the melting temperature ( $T_m$  plasticized starch) and the melting enthalpy ( $\Delta H_m$   
125 plasticized starch) linked to the plasticized starch fraction, it is possible to verify a slight  
126 interaction between pine resins derivatives and the plasticized starch fraction of the  
127 formulations. The melting temperature decreased in about 4 °C for the formulations that  
128 contains LF and UT, and 7 °C in the MaterBi-GR based formulations. This is an  
129 indicative that GR has a better plasticizing effect on the Mater-Bi®, than the chemically  
130 modified resins (LF and UT). The melting enthalpy has a similar behaviour, which  
131 trends to decrease more evidently in the UT and GR added formulations. This explains  
132 the difference between the interactions of LF and UT, and the interaction of GR with the  
133 Mater-Bi® matrix. On one hand, LF has mainly a marked cohesive effect on Mater-  
134 Bi®, and UT has both effects, plasticizing and cohesive, already advised on the  
135 mechanical properties. On the other hand, GR confers a marked  
136 plasticization/compatibilizing effect, even greater than the other resins derivatives, with  
137 influence in the mechanical, thermal and morphological properties of the formulations  
138 based on MaterBi-GR blends.

139 Finally, regarding the crystallization temperature ( $T_c$ ), it is possible to observe that  
140 ormulations show a noticeable decrement in this transition temperature that reaches 5.6,  
141 10.8 and 16 °C with LF, UT and GR at 15wt.%, respectively. Meanwhile, no significant  
142 changes were observed on the crystallization enthalpy ( $\Delta H_c$ ) for all formulations.

143



144

145

**Figure 7.** a) DSC second heating and b) DSC cooling of neat Mater-Bi® and

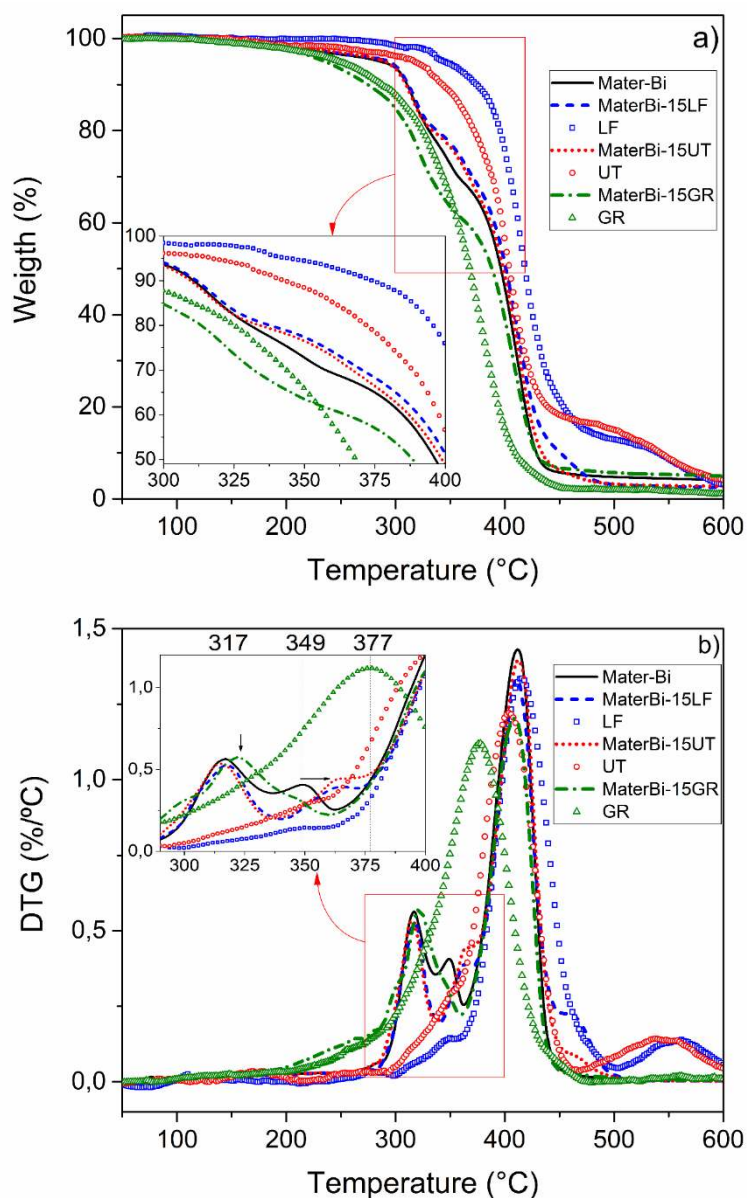
146

formulations with 15 wt.% of pine resin derivatives

147 **Table 4.** DSC thermal properties of neat Mater-Bi® and Mater-Bi®-pine resin derivatives formulations

Formulation	DSC second heating								DSC Cooling		
	T <sub>g</sub> (°C)	T <sub>mPCL</sub> (°C)	T <sub>cc</sub> (°C)	ΔH <sub>cc</sub> (J/g)	T <sub>mPBAT</sub> (°C)	ΔH <sub>mPBAT</sub> (J/g)	T <sub>m plasticized starch</sub> (°C)	ΔH <sub>m plasticized starch</sub> (J/g)	X <sub>c</sub> (%)	T <sub>c</sub> (°C)	ΔH <sub>c</sub> (J/g)
Mater-Bi®	-32.0	56.3	107.3	2.2	127.9	2.3	150.3	2.5	0.1	92.5	9,2
MaterBi-5LF	-31.0	56.3	-	-	126.4	3.0	146.1	2.6	1.8	88.0	10.2
MaterBi-10LF	-29.1	56.5	-	-	123.9	3.6	146.6	2.1	2.0	86.9	11.1
MaterBi-15LF	-27.7	56.6	-	-	123.7	3.5	146.6	2.1	1.8	88.2	8.5
MaterBi-5UT	-29.7	57.3	-	-	124.2	3.7	147.4	2.1	2.2	86.6	9.5
MaterBi-10UT	-27.0	56.6	-	-	119.9	6.0	148.5	1.1	3.3	83.3	10.7
MaterBi-15UT	-27.0	56.4	-	-	118.9	5.9	147.6	1.0	3.1	81.7	9.5
MaterBi-5GR	-28.6	56.2	-	-	123.9	1.8	144.6	3.1	1.1	84.6	12.3
MaterBi-10GR	-25.3	54.1	-	-	122.4	2.6	142.8	2.5	2.4	82.9	9.9
MaterBi-15GR	-22.3	53.6	-	-	111.6	5.4	143.0	1.3	2.8	76.6	8.2

148 Regarding TGA analysis, **Figure 8-a** shows the thermogravimetric curves of  
149 neat Mater-Bi® and the formulations added with 15 wt.% of resin. Meanwhile, **Table 5**  
150 summarizes the thermal data of the initial degradation temperature (5% of weight loss,  
151  $T_{5\%}$ ) as well as the maximum degradation peaks ( $T_{max}$ ), extracted from the TGA and  
152 DTG curves, respectively.  
153



154  
155 **Figure 8. a)** TGA and **b)** DTG curves of Mater-Bi® and formulations with 15 wt.% of  
156 pine resin derivatives.

157 The results showed that the polymeric matrix used in this study (Mater-Bi®) presents a  
158 three step degradation process: the first step centred at 317 °C, corresponding to the  
159 plasticized starch degradation.<sup>19,21,48,61</sup> The second step centred at 349 °C, attributed to  
160 either the degradation of the compatibilizing agents usually present in Mater-Bi®  
161 formulations, or to interpenetrating networks formed by starch with the aliphatic  
162 aromatic polyesters.<sup>61</sup> The third step, with a maximum degradation peak at 412 °C,  
163 corresponding to the degradations of the PBAT.<sup>19</sup> This peak could be overlapped with  
164 the degradation peak of PCL, because it has similar degradation temperature<sup>53</sup> and also  
165 because its fraction on Mater-Bi® is less than 10 wt.%.<sup>5</sup> The  $T_{5\%}$  increased up to 4 °C  
166 and 7 °C in formulations added with UT or LF, respectively. On the contrary, in GR  
167 added formulations, the onset degradation temperature had a noticeable decrement  
168 between 14 °C (in MaterBi-5GR formulation) and 51 °C (in MaterBi-15GR formulation)  
169 compared to neat Mater-Bi®. This behaviour is attributed to the inherent thermal  
170 characteristics of each pine resin derivative, where GR started the degradation at lower  
171 temperatures than LF or UT, because pentaerythritol esters of gum rosin present a more  
172 thermally stable chemical structure and also interact better with the polymeric matrix by  
173 hydrogen bonding interactions leading to a stabilizing effect which protect the  
174 polymeric matrix from thermal degradation.

175 As discussed for the neat Mater-Bi®, all formulations exhibit a three-step  
176 degradation. The maximum degradation temperatures ( $T_{max}$ ) presented the following  
177 behaviours:  $T_{max1}$  increased their values in MaterBi-GR formulations, while LF and UT  
178 did not modify these temperatures. Besides,  $T_{max2}$  tend to increase its values up to 18 °C  
179 in MaterBi-10LF and MaterBi-5UT. In contrast, for GR added formulations, the peak  
180 corresponding to  $T_{max1}$  was overlapped with the peak corresponding to  $T_{max2}$ . This  
181 behaviour reveals that GR had somewhat interaction with the plasticized starch portion

182 of the Mater-Bi® than LF and UT. However, the thermal stability of the formulations  
183 added with GR tends to decrease, and those with chemically modified resins, LF and  
184 UT, tends to increase. On the other hand, the addition of resins did not influence the  
185 degradation step corresponding to PBAT portion of the polymeric material ( $T_{max3}$ ), even  
186 though the tendency of this temperature is to decrease in higher GR resin contents. As  
187 well in the DTG curves, shown in **Figure 8-b**, it is important to notice that MaterBi-  
188 15LF and MaterBi-15UT curves presented a peak near to 460 °C due to the resin  
189 remainder in the formulations, as can be seen from the DTG of neat pentaerythritol ester  
190 of colophony.<sup>31</sup>

191

192 **Table 5.** Onset degradation temperature ( $T_{5\%}$ ), temperatures of the maximum  
 193 decomposition rate ( $T_{\max 1}$ ,  $T_{\max 2}$  and  $T_{\max 3}$ ) for all formulations studied

Formulation	$T_{5\%}$ (°C)	$T_{\max 1}$ (°C)	$T_{\max 2}$ (°C)	$T_{\max 3}$ (°C)
Mater-Bi®	286	317	349	412
MaterBi-5LF	286	317	346	411
MaterBi-10LF	292	316	366	411
MaterBi-15LF	293	318	365	411
LF	345	-	415	561
MaterBi-5UT	287	316	367	410
MaterBi-10UT	290	317	358	411
MaterBi-15UT	290	315	365	412
UT	317	-	404	545
MaterBi-5GR	272	320	-	411
MaterBi-10GR	253	321	350	411
MaterBi-15GR	235	322	-	409
GR	248	-	377	-

194

195 Finally, **Table 3** shows the Heat Deflection Temperature (HDT) where is  
 196 possible to verify that this property followed the same tendency of the already discussed  
 197 properties. LF resin did not change significantly the HDT. In fact, Mater-Bi® chains did  
 198 not have easy movement, due to the low compatibilizing effect of the LF resin. This  
 199 behaviour also allowed confirming the lack of the plasticizing effect of LF. Whereas,  
 200 adding 10 wt.% of GR or 15 wt.% of UT, the HDT at room temperature was reduced,

201 confirming their important plasticizing effect, since those resins facilitates the free  
202 movements of the polymer chains.

203

### 204 3.6. Dynamic-Mechanical properties

205

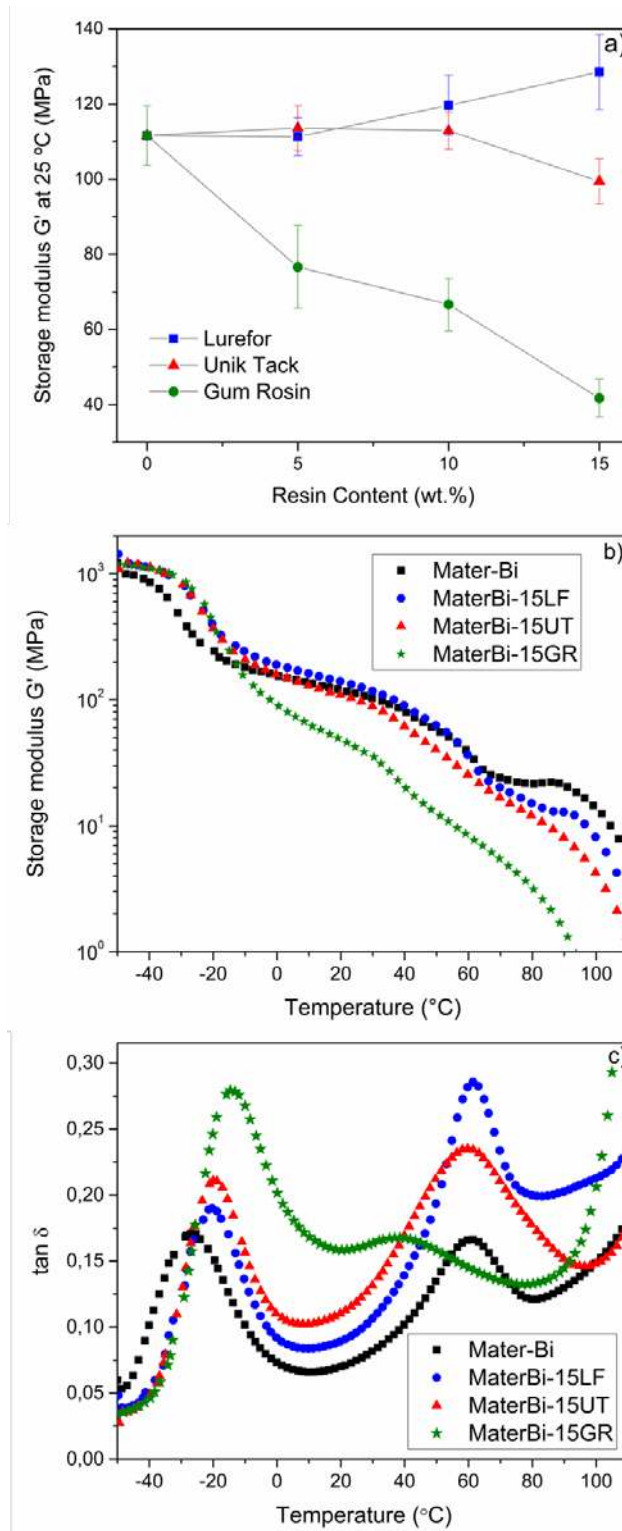
206 The effect of pine resin derivatives on the dynamic-mechanical properties of  
207 Mater-Bi® was also studied. **Figure 9** presents the trend of storage modulus of Mater-  
208 Bi®-based formulations respect to the resin type and content (**Figure 9-a**), the evolution  
209 of storage modulus ( $G'$ ) and the gap between the loss modulus ( $G''$ ) and  $G'$ ,  
210 represented by the tangent of the gap ( $\tan \delta$ ), plotted against the temperature (**Figure 9-**  
211 **b** and **Figure 9-c**, respectively). Considering the amount of resin added, the storage  
212 modulus determined at 25 °C follows the same trend than Young's modulus (**Figure 2-**  
213 **a**) and flexural modulus (**Figure 3-a**). As discussed, LF and UT resins has a  
214 compatibilizing effect between the resin and the polymeric matrix, while UT resin also  
215 shows a plasticizing effect. On the other hand, increasing the amount of GR there is a  
216 linear decrement in the storage modulus values, suggesting a solubilising,  
217 compatibilizing and plasticizing effect. Plus, if the trend of storage modulus ( $G'$ ) with  
218 temperature (**Figure 9-b**) is observed, in the curve corresponding to the neat Mater-  
219 Bi®, two important losses of  $G'$  are observed.<sup>17</sup> The first one corresponds to the  
220 combination of the glass transition of the PBAT and the one of the plasticized starch  
221 portion of the Mater-Bi® ( $T_{gPBAT}$  and  $T_{g\text{ plasticized starch}}$ ) having associated a peak in  $\tan \delta$   
222 at -28 °C.<sup>19</sup> The second major loss of  $G'$  is associated with a peak of  $\tan \delta$  at 60 °C,  
223 corresponding to the PCL and additives portion which represents the 10% of the Mater-  
224 Bi® polymeric matrix, as discussed before on FTIR and DSC analysis.<sup>55</sup> Thus, in these  
225 dynamic mechanical analyses it was observed a peak around 60 °C that coincides with



226 the melting temperature of the PCL.<sup>18,57</sup> Below the first  $T_g$  ( $T_{gPBAT}$  and  $T_{g\text{ plasticized starch}}$ ),  
227 Mater-Bi® formulations with 15 wt.% of UT, LF and GR have a higher  $G'$  value than  
228 the neat Mater-Bi®. In addition, above this  $T_g$ , the formulations containing 15 wt.% of  
229 UT and LF provide higher  $G'$  values, increasing the values of the elastic component of  
230 polymeric matrix. This is due to the chemical interaction between resin derivatives and  
231 Mater-Bi® components. Moreover, this behaviour contributes to a greater cohesion  
232 between the components of the Mater-Bi®, already observed in other properties. This  
233 interaction may be due to the molecules of both chemically modified resins act as  
234 compatibilizer agent, hindering molecular movement of the polymeric chains.  
235 However, the formulation with 15 wt.% of GR showed values of  $G'$  below to those  
236 obtained for neat Mater-Bi®. In this case, GR acts as a compatibilizing agent between  
237 the components of matrix (plasticized starch, PBAT and PCL), increasing the  
238 intramolecular free volume and the solubility between them.<sup>6,19</sup> This causes a lower  
239 interaction between the functional groups of the polymer chains and increases the  
240 viscous component of the Mater-Bi® and consequently its fluidity. Moreover, the  
241 processability of the Mater-Bi®-resin based formulations is easier than that of neat  
242 Mater-Bi®, standing out the MaterBi-GR based formulations.

243         Analysing the effect of  $\tan \delta$  peaks (**Figure 9-c**) of Mater-Bi® added with pine  
244 resin derivatives it is possible to corroborate the effect of the LF, UT and GR resins on  
245 the matrix. As observe from DSC results, LF and UT act as cohesive agents, probably  
246 as a consequence of the chemical interactions between the functional groups of the  
247 polymer components and the functional groups of the modified resin derivatives  
248 commented in FTIR analysis.<sup>3,5,22</sup> In fact, the peak of  $T_{gPBAT}$ - $T_{g\text{ plasticized starch}}$  (between -  
249 20 and -25 °C) was well defined and separated from that corresponding to the melting of  
250 PCL (around 60 °C).<sup>57</sup> In contrast, the MaterBi-GR based formulations exhibited a very

251 different behaviour: firstly, the peak corresponding to  $T_{g\text{PBAT}}-T_{g\text{ plasticized starch}}$  was shifted  
252 to higher temperatures (15 °C in the MaterBi-15GR). These shifts indicate an  
253 improvement in the interfacial adhesion between the components of the neat Mater-Bi®  
254 and the resins.<sup>19</sup> Secondly, the peak of PCL component at 60 °C disappeared. The  
255 second peak of the MaterBi-15GR curve correspond to the melting of GR. The  
256 disappearance of the melting peak is due to the greater compatibilizing effect of the GR  
257 resin on the components of Mater-Bi®. Furthermore, said effect results in a large  
258 increase in the solubility of the three polymeric fractions of the Mater-Bi®, which  
259 increased their miscibility between them due to the GR presence in addition to an  
260 important plasticizing effect. Finally, these results are in good agreement with the easier  
261 processability of the Mater-Bi®-resin based formulations, the lower Shore D hardness  
262 as well as the lower melting temperature of the MaterBi-GR based formulations which  
263 are indicatives of the compatibilizing-plasticizer effect of the GR in the Mater-Bi®  
264 matrix.  
265



266

267 **Figure 9.** DMA analysis: a) Effect of increasing amount of pine resin derivatives on the

268 storage modulus of Mater-Bi®-based formulations at 25 °C; b) storage modulus

269 and c) loss factor curves for neat Mater-Bi® and 15 wt.% of pine resin

270 derivatives formulations

271

#### 272 **4. Conclusions**

273

274 Mater-Bi®-resin based formulations were successfully processed by melt  
275 extrusion followed by injection moulding process. Mater-Bi® was blended with three  
276 pine resin derivatives which act in three different ways. GR exerts a marked  
277 plasticizing, solubilizing and compatibilizing effect on the Mater-Bi® polymeric matrix.  
278 That means, an increase of 365% in maximum elongation at break, 480% in toughness  
279 and 250% in the Charpy's impact energy, in material formulated with 15 wt.% of GR.  
280 There is also a significant decrease on the processing temperatures, up to 50 °C lower  
281 than the processing temperatures of neat Mater-Bi®. On the other hand, chemically  
282 modified resins showed different behaviour. LF acts as a compatibilizer between the  
283 components of Mater-Bi® (PBAT, plasticized starch and PCL), contributing up to  
284 250% more toughness to the material, 5% more Young's modulus and 13% more tensile  
285 strength in formulations with 10 wt.% of LF resin, with respect to neat Mater-Bi®.  
286 Meanwhile, UT acts as a compatibilizer/plasticizer agent, which confers greater  
287 cohesion to the components of the Mater-Bi®, improving its processability performance  
288 by decreasing the processing temperature up to 45 °C and increasing the maximum  
289 elongation at break by 72% in formulations with 15 wt.% of UT resin. Additionally,  
290 SEM micrographs and the changes in thermal transitions corroborated the plasticizing  
291 solubilising and cohesive behaviour observed in each formulation. Moreover, pine  
292 resins and their derivatives are a viable alternative as natural additives for Mater-Bi®  
293 (composed by plasticized starch, aliphatic/aromatic polyesters and aliphatic polyesters  
294 as components). Finally, the processability properties conferred by the rosin resins  
295 studied here opens the possibility of using these formulations in several industrial  
296 applications such as food packaging, agricultural mulch films or greenhouse plastics.

297 **Acknowledgment**

298

299 This work has been supported by the Spanish Ministry of Economy and  
300 Competitiveness, PROMADEPCOL (MAT2017-84909-C2-2-R). M.P. Arrieta thanks  
301 Complutense University of Madrid for "Ayudas para la contratación de personal  
302 postdoctoral en formación en docencia e investigación en departamentos de la UCM".

303

304 **References**

305

- 306 1. Plastics Europe, Plastics – the Facts 2016. An analysis of European plastics  
307 production, demand and waste data” [Online]. Available:  
308 <http://www.plasticseurope.es/industria-del-plastico/datos-de-mercado.aspx>. 2017.
- 309 2. Arrieta, M. P.; Peponi, L.; López, D.; Fernández-García, M., Industrial Crops and  
310 Products 111, 317 2018.
- 311 3. Akrami, M.; Ghasemi, I.; Azizi, H.; Karrabi, M.; Seyedabadi, M., Carbohydrate  
312 polymers 144, 254 2016.
- 313 4. Arrieta, M. P.; Samper, M. D.; Aldas, M.; López, J., Materials 10, 1008 2017.
- 314 5. Borchani, K. E.; Carrot, C.; Jaziri, M., Composites Part A: Applied Science and  
315 Manufacturing 78, 371 2015.
- 316 6. Ferri, J. M.; Garcia-Garcia, D.; Sánchez-Nacher, L.; Fenollar, O.; Balart, R.,  
317 Carbohydrate polymers 147, 60 2016.
- 318 7. Arrieta, M. P.; López, J.; López, D.; Kenny, J. M.; Peponi, L., Polymer  
319 Degradation and Stability 132, 145 2016.
- 320 8. Fabra, M. J.; López-Rubio, A.; Cabedo, L.; Lagaron, J. M., Journal of Colloid and  
321 Interface Science 483, 84 2016.

- 322 9. Makaremi, M.; Pasbakhsh, P.; Cavallaro, G.; Lazzara, G.; Aw, Y. K.; Lee, S. M.;  
323 Milioto, S., *ACS applied materials & interfaces* 9, 17476 2017.
- 324 10. Niu, X.; Liu, Y.; Song, Y.; Han, J.; Pan, H., *Carbohydrate polymers* 183, 102  
325 2018.
- 326 11. Mujica-Garcia, A.; Sonseca, A.; Arrieta, M. P.; Yusef, M.; López, D.; Gimenez,  
327 E.; Kenny, J. M.; Peponi, L. In *Advanced Surface Engineering Materials*, 2016.
- 328 12. Sessini, V.; Arrieta, M. P.; Kenny, J. M.; Peponi, L., *Polymer Degradation and*  
329 *Stability* 132, 157 2016.
- 330 13. Ferri, J. M.; Garcia-Garcia, D.; Carbonell-Verdu, A.; Fenollar, O.; Balart, R.,  
331 *Journal of Applied Polymer Science* 135 2018.
- 332 14. Trovatti, E.; Carvalho, A. J. F.; Gandini, A., *Polymer International* 64, 605 2015.
- 333 15. Samper-Madrigal, M.; Fenollar, O.; Dominici, F.; Balart, R.; Kenny, J., *Journal of*  
334 *materials science* 50, 863 2015.
- 335 16. Azevedo, V. M.; Borges, S. V.; Marconcini, J. M.; Yoshida, M. I.; Neto, A. R. S.;  
336 Pereira, T. C.; Pereira, C. F. G., *Carbohydrate polymers* 157, 971 2017.
- 337 17. Sessini, V.; Raquez, J. M.; Lourdin, D.; Maigret, J. E.; Kenny, J. M.; Dubois, P.;  
338 Peponi, L., *Macromolecular Chemistry and Physics* 218 2017.
- 339 18. Correa, A. C.; Carmona, V. B.; Simão, J. A.; Mattoso, L. H. C.; Marconcini, J.  
340 M., *Carbohydrate polymers* 167, 177 2017.
- 341 19. Lendvai, L.; Apostolov, A.; Karger-Kocsis, J., *Carbohydrate polymers* 173, 566  
342 2017.
- 343 20. Mikus, P.-Y.; Alix, S.; Soulestin, J.; Lacrampe, M.; Krawczak, P.; Coqueret, X.;  
344 Dole, P., *Carbohydrate polymers* 114, 450 2014.
- 345 21. Sessini, V.; Arrieta, M. P.; Raquez, J. M.; Dubois, P.; Kenny, J. M.; Peponi, L.,  
346 *Polymer Degradation and Stability* 159, 184 2019.

- 347 22. Arrieta, M. P.; Samper, M. D.; Jiménez-López, M.; Aldas, M.; López, J.,  
348 Industrial Crops and Products 99, 196 2017.
- 349 23. Narayanan, M.; Loganathan, S.; Valapa, R. B.; Thomas, S.; Varghese, T.,  
350 International Journal of Biological Macromolecules 99, 37 2017.
- 351 24. Wilbon, P. A.; Chu, F.; Tang, C., Macromolecular rapid communications 34, 8  
352 2013.
- 353 25. Rodríguez-García, A.; Martín, J. A.; López, R.; Sanz, A.; Gil, L., Industrial Crops  
354 and Products 86, 143 2016.
- 355 26. Sharma, L.; Singh, C., Polymer Composites 39, 1480 2018.
- 356 27. Moustafa, H.; El Kissi, N.; Abou-Kandil, A. I.; Abdel-Aziz, M. S.; Dufresne, A.,  
357 ACS applied materials & interfaces 9, 20132 2017.
- 358 28. Romero, A. in Atelier International de diagnostique de l'industrie des résineux de  
359 seconde transformation: 2012.
- 360 29. Yu, C.; Chen, C.; Gong, Q.; Zhang, F. A., Polymer International 61, 1619 2012.
- 361 30. Gutierrez, J.; Tercjak, A., RSC Advances 4, 32024 2014.
- 362 31. Cavallaro, G.; Lazzara, G.; Milioto, S.; Parisi, F.; Ruisi, F., Cellulose 24, 3367  
363 2017.
- 364 32. Arrieta, M. P.; López, J.; Ferrándiz, S.; Peltzer, M. A., Acta Horticulturae 1065,  
365 719 2015.
- 366 33. Arrieta, M. P.; López, J.; Hernández, A.; Rayón, E., European Polymer Journal  
367 50, 255 2014.
- 368 34. Liu, X. Q.; Huang, W.; Jiang, Y. H.; Zhu, J.; Zhang, C. Z., Express Polymer  
369 Letters 62012.
- 370 35. López, J.; Arrieta, M. P., Actas del II Simp. Int. Resinas Nat., 206 2013.

- 371 36. International Standards Organization, ISO 527-1:2012 - Plastics - Determination  
372 of tensile properties - Part 1: General. 2012.
- 373 37. Sessini, V.; Raquez, J. M.; Lo Re, G.; Mincheva, R.; Kenny, J. M.; Dubois, P.;  
374 Peponi, L., ACS Applied Materials and Interfaces 8, 19197 2016.
- 375 38. Samper, M. D.; Bartomeu, D.; Arrieta, M. P.; Ferri, J. M.; López-Martínez, J.,  
376 Materials 112018.
- 377 39. International Standards Organization, ISO 178:2010 - Plastics - Determination of  
378 flexural properties. 2010.
- 379 40. International Standards Organization, ISO 179:2010 - Plastics - Determination of  
380 charpy impact properties. 2010.
- 381 41. International Standards Organization, ISO 868:2003 - Plastics and ebonite -  
382 Determination of indentation hardness by means of a durometer (Shore hardness).  
383 2003.
- 384 42. Jost, V., Express Polymer Letters 12, 429 2018.
- 385 43. International Standards Organization, ISO 75-1:2013 - Plastics - Determination of  
386 temperature of deflection under load - Part 1: General test method. 2013.
- 387 44. Mok, S. L.; Kwong, C. K.; Lau, W. S., The International Journal of Advanced  
388 Manufacturing Technology 18, 404 2001.
- 389 45. Al-Itry, R.; Lamnawar, K.; Maazouz, A., Polymer Degradation and Stability 97,  
390 1898 2012.
- 391 46. Bastioli, C.; Cerutti, A.; Guanella, I.; Romano, G. C.; Tosin, M., Journal of  
392 Polymers and the Environment 3, 81 1995.
- 393 47. Esmacili, M.; Pircheraghi, G.; Bagheri, R., Polymer International 66, 809 2017.
- 394 48. Mano, J.; Koniarova, D.; Reis, R., Journal of Materials Science: Materials in  
395 Medicine 14, 127 2003.



- 396 49. Khan, G.; Yadav, S. K.; Patel, R. R.; Kumar, N.; Bansal, M.; Mishra, B.,  
397 International Journal of Biological Macromolecules 103, 1311 2017.
- 398 50. Arrieta, M. P.; Peponi, L., European Polymer Journal 89, 174 2017.
- 399 51. Jindal, R.; Sharma, R.; Maiti, M.; Kaur, A.; Sharma, P.; Mishra, V.; Jana, A.,  
400 Polymer Bulletin 74, 2995 2017.
- 401 52. Singh, V.; Joshi, S.; Malviya, T., International Journal of Biological  
402 Macromolecules 112, 390 2018.
- 403 53. Garcia-Garcia, D.; Rayón, E.; Carbonell-Verdu, A.; Lopez-Martinez, J.; Balart,  
404 R., European Polymer Journal 86, 41 2017.
- 405 54. Peponi, L.; Sessini, V.; Arrieta, M. P.; Navarro-Baena, I.; Sonseca, A.; Dominici,  
406 F.; Gimenez, E.; Torre, L.; Tercjak, A.; López, D.; Kenny, J. M., Polymer  
407 Degradation and Stability 151, 36 2018.
- 408 55. Muthuraj, R.; Misra, M.; Mohanty, A., Journal of Applied Polymer Science  
409 1322015.
- 410 56. Signori, F.; Coltelli, M.-B.; Bronco, S., Polymer Degradation and Stability 94, 74  
411 2009.
- 412 57. Navarro-Baena, I.; Arrieta, M. P.; Sonseca, A.; Torre, L.; López, D.; Giménez, E.;  
413 Kenny, J. M.; Peponi, L., Polymer Degradation and Stability 121, 171 2015.
- 414 58. Salgado, C.; Arrieta, M. P.; Peponi, L.; Fernández-García, M.; López, D.,  
415 Macromolecular Materials and Engineering 3022017.
- 416 59. Zhao, P.; Liu, W.; Wu, Q.; Ren, J., Journal of Nanomaterials 2010, 4 2010.
- 417 60. Ferri, J. M.; Fenollar, O.; Jorda-Vilaplana, A.; García-Sanoguera, D.; Balart, R.,  
418 Polymer International 65, 453 2016.
- 419 61. Cerruti, P.; Santagata, G.; d'Ayala, G. G.; Ambrogio, V.; Carfagna, C.;  
420 Malinconico, M.; Persico, P., Polymer Degradation and Stability 96, 839 2011.

421

422